HHS Public Access

Author manuscript

Clin Cancer Res. Author manuscript; available in PMC 2017 February 15.

Published in final edited form as:

Clin Cancer Res. 2016 August 15; 22(16): 4236–4248. doi:10.1158/1078-0432.CCR-15-2614.

OX40$^+$ regulatory T cells in cutaneous squamous cell carcinoma suppress effector T cell responses and associate with metastatic potential

Chester Lai[1,2], **Suzannah August**[1,2], **Amel Albibas**[1], **Ramnik Behar**[1], **Shin-Young Cho**[1], **Marta E Polak**[1], **Jeff Theaker**[3], **Amanda S MacLeod**[4], **Ruth R French**[5], **Martin J Glennie**[5], **Aymen Al-Shamkhani**[5], and **Eugene Healy**[1,2]

[1]Dermatopharmacology, Clinical and Experimental Sciences, Faculty of Medicine, University of Southampton, Southampton, UK

[2]Dermatology, University Hospital Southampton NHS Foundation Trust, Southampton, UK

[3]Histopathology, University Hospital Southampton NHS Foundation Trust, Southampton, UK

[4]Dermatology, Duke University Medical Center, Durham, NC, USA

[5]Cancer Sciences, Faculty of Medicine, University of Southampton, Southampton, UK

Abstract

Purpose—Cutaneous squamous cell carcinoma (cSCC) is the most common human cancer with metastatic potential. Despite T cells accumulating around cSCCs, these tumors continue to grow and persist. To investigate reasons for failure of T cells to mount a protective response in cSCC, we focused on regulatory T cells (Tregs) as this suppressive population is well represented among the infiltrating lymphocytes.

Experimental Design—Flow cytometry was conducted on cSCC lymphocytes and *in vitro* functional assays were performed using sorted tumoral T cells. Lymphocyte subsets in primary cSCCs were quantified immunohistochemically.

Results—FOXP3$^+$ Tregs were more frequent in cSCCs than in peripheral blood ($p<0.0001$, n=86 tumors). Tumoral Tregs suppressed proliferation of tumoral effector CD4$^+$ ($p=0.005$, n=10 tumors) and CD8$^+$ T cells ($p=0.043$, n=9 tumors) and inhibited interferon-γ secretion by tumoral effector T cells ($p=0.0186$, n=11 tumors). The costimulatory molecule OX40 was expressed predominantly on tumoral Tregs ($p<0.0001$, n=15 tumors) and triggering OX40 with an agonist anti-OX40 antibody overcame the suppression exerted by Tregs, leading to increased tumoral effector CD4$^+$ lymphocyte proliferation ($p=0.0098$, n=10 tumors). Tregs and OX40$^+$ lymphocytes were more abundant in primary cSCCs which metastasized than in primary cSCCs which had not metastasized (n=48 and n=49 tumors respectively).

Corresponding author: Professor Eugene Healy, Dermatopharmacology, University of Southampton, Sir Henry Wellcome Laboratories, Southampton General Hospital, Southampton, Hampshire, SO16 6YD, UK. Tel: +44(0)2380795232; ehealy@soton.ac.uk.

Conflict of interest: The authors declare no conflict of interest.

Conclusions—Tregs in cSCCs suppress effector T cell responses and are associated with subsequent metastasis, suggesting a key role for Tregs in cSCC development and progression. OX40 agonism reversed the suppressive effects of Tregs *in vitro*, suggesting that targeting OX40 could benefit the subset of cSCC patients at high risk of metastasis.

Introduction

Non melanoma skin cancer (NMSC), which comprises cutaneous squamous cell carcinomas (cSCCs) and basal cell carcinomas (BCCs), is the most common type of cancer and greatly impacts on global health, with estimated annual incidences of 2.8 million cSCCs and 10 million BCCs worldwide (1). In the USA alone, 3.5 million NMSCs arise each year, with cSCCs accounting for 700,000 of these tumors (2). Skin cancer creates a substantial economic burden and, in 2004, the estimated cost of skin cancer and precancerous skin lesions to US health services was $6.6 million (3). Despite treatment with surgery, cSCC poses problems because of its propensity to metastasize, occurring in 16 – 30% of tumors which have invaded 6mm in depth or over 2 cm in diameter (4, 5).

cSCCs are keratinocyte-derived neoplasms associated with chronic exposure to ultraviolet radiation, which causes genetic alterations within the epidermis and promotes squamous cell carcinogenesis and subsequent metastases (6–8). Alterations in immunity have a key role in regulating cutaneous carcinogenesis, as evidenced by immunosuppression greatly increasing the incidence of cSCCs, with these tumors 65–250 fold more frequent in organ transplant recipients (9). Indeed, cSCC constitutes an ideal tumor model for investigating cancer immunology because most cSCCs are surrounded by an immune cell infiltrate, yet this infiltrate is generally incapable of mounting a successful anti-tumor response. Tregs have a physiological function in maintaining immunological self-tolerance and homeostasis, however, in certain cancers increased numbers of tumor infiltrating Tregs are associated with poorer clinical outcome, suggesting that Tregs suppress immune responses within the tumoral environment (10–13). As a result of this, there has been considerable interest in developing immunotherapeutic strategies that target Tregs and boost effector immune responses in cancer (14–18). One such approach involves the provision of costimulatory signals through receptors that belong to the tumor necrosis receptor superfamily, including OX40. Engagement of this receptor has been shown to promote T cell activation through effects on different subpopulations of T cells, for example by promoting proliferation and survival of effector memory T cells following antigenic activation, as well as by suppressing regulatory T cell activity (16–19). These effects highlight OX40 as a promising target for tumor therapy, and cases of tumor regression have been recently reported in a phase I clinical trial with anti-OX40 agonistic antibody (20).

In this study, we show that cSCCs contain a higher proportion of Tregs than peripheral blood from the same individuals, and that these tumoral Tregs suppress tumoral effector T cell proliferation and interferon-γ secretion. In addition, increased expression of the costimulatory receptor OX40 was noted on cSCC Tregs and activation of OX40 enhanced tumoral $CD4^+$ effector T cell responses. Furthermore, increased frequencies of Tregs and $OX40^+$ lymphocytes are observed in primary cSCCs which subsequently metastasize. The

results demonstrate that $OX40^+$ Tregs in cSCCs are immunosuppressive and are associated with a propensity of cSCCs to metastasize.

Materials and Methods

Immunohistochemistry

Ethical approval for the study was provided by the South Central Hampshire B NRES Committee (reference number 07/H0504/187). Archived formalin-fixed paraffin-embedded (FFPE) cSCC samples were obtained from University Hospital Southampton NHS Foundation Trust. Immunohistochemistry was performed as described previously (21), with microwave antigen retrieval performed in either 10 μM citrate or 1.6 μM EDTA buffers. Primary antibodies included anti-CD3 (1:200, DAKO), anti-CD4 (1:100, DAKO), anti-CD8 (1:20, Abcam), anti-CD25 (1:50, Novocastra), anti-FOXP3 (1:50, Abcam) and anti-OX40 (1:50, BD Biosciences), and biotinylated goat anti-mouse (1:200, DAKO) or swine anti-rabbit (1:400, DAKO) were used as secondary antibodies. For cell quantification, 5 representative images at 40× magnification were taken from each immunostained cSCC section and analysed using ImageJ software.

Immunofluorescence/confocal microscopy

Tissue from freshly excised cSCC was obtained from patients during surgery at the Dermatology Department, University Hospital Southampton NHS Foundation Trust. The tissue samples (n=15 tumors) were snap frozen in liquid nitrogen, embedded in OCT medium, cryosectioned and immunostained as described previously (22). Primary antibodies included anti-CD3 (1:200, DAKO), anti-CD4 (1:50, Abcam), anti-CD8 (1:20, Invitrogen), anti-FOXP3 (1:20, eBioscience), anti-cytokeratin 16 (1:20, Thermo Scientific), anti-cytokeratin 17 (1:20, DAKO), anti CD31 (1:200, eBioscience), anti-CLA (1:200, Biolegend), anti-E-selectin (1:20, R & D Systems) and anti-OX40 (1:200, BD Biosciences). Fluorophore conjugated secondary antibodies comprised Alexa Fluor 488 goat anti-mouse IgG1a, Alexa Fluor 488 goat anti-rat IgM, Alexa Fluor 555 goat anti-rabbit IgG, Alexa Fluor 555 goat anti-rat IgG and Alexa Fluor 633 goat anti-mouse IgG2a (all from Invitrogen). Tissue sections were counterstained with DAPI (Sigma) before being mounted in Mowiol 4–88 (Harco) and imaged using a Zeiss Axioskop 2 fluorescence microscope or a Leica SP5 confocal microscope.

Lymphocyte isolation/flow cytometry

Following formal surgical excision of the cSCC (n=93 tumors), part of the fresh tumor sample was taken and cut into small pieces, then enzymatically digested with 1 mg/ml collagenase I-A (Sigma) and 10 μg/ml DNAse I (Sigma) in RPMI medium (Gibco) at 37°C for 1.5 hours. The resulting suspension was passed through 70μm cell strainers (BD) and centrifuged in Optiprep (Axis-Shield). Peripheral blood mononuclear cells (PBMCs) were isolated from venous blood from the cSCC patients by centrifugation with Lymphoprep (Axis-Shield). The following fluorophore conjugated antibodies were used for flow cytometry: anti-CD3 (APC Cy7, Biolegend), anti-CD4 (PerCP Cy5.5 or FITC, Biolegend), anti-CD8 (PE Cy7, Biolegend), anti-CD25 (PE, Invitrogen), anti-CD127 (Brilliant Violet 421, Biolegend), anti-FOXP3 (APC, eBioscience), anti-CD45RO (PerCP Cy5.5, Biolegend),

anti-Helios (PerCP Cy5.5, Biolegend), anti-CLA (Brilliant Violet 421, BD Biosciences), anti-CCR4 (PerCPCy5.5, Biolegend or FITC, R&D Systems) and anti-OX40 (PE, eBioscience). For cell surface staining, cells were incubated with the antibodies in the dark for 30 minutes at 4°C in PBS + 1% BSA + 10% FBS. For intracellular markers, a FOXP3 staining buffer set (eBioscience) was used to fix and permeabilize cells prior to staining (23, 24). An aqua live/dead viability stain (Invitrogen) was added before flow cytometry using a BD FACSAria.

Generation of anti-human OX40 monoclonal antibodies (mAb)

For the production of anti-hOX40 mAb, mice were immunized with hOX40-hFc fusion protein and 293F cells transfected with hOX40 (primary fusion protein in complete Freund's adjuvant, s.c.; secondary transfected cells in incomplete, s.c.; final boost fusion protein, i.v.). Spleen cells from the immunized mice were fused with NS-1 cells using conventional hybridoma technology. Plates were screened by ELISA using hOX40-hFC fusion protein and positive wells tested for binding to hOX40-transfected 293F cells. Agonist mAb were identified by their ability to enhance T cell proliferation using cultured peripheral blood mononuclear cells obtained from healthy volunteers that were stimulated with sub-optimal concentrations of anti-CD3 mAb.

Functional assays

Tumoral $CD3^+CD4^+CD25^{high}CD127^{low}$ Tregs and $CD3^+CD4^+CD25^{low}$ or $CD3^+CD8^+$ effector T cells were sorted by FACS using the "purity" setting. 96 well U-bottomed plates were used for co-culture assays and all functional experiments were performed using triplicate wells. Tumoral effector T cells (2,500 per well) were co-cultured with/without tumoral Tregs (1,250 per well) in the presence of irradiated (47Gy) autologous PBMCs (25,000 per well), stimulated with 1 μg/ml phytohemagglutinin (PHA, Sigma) or 1 μg/ml soluble anti-CD3 (eBioscience). After culture for 48 hours, tritiated thymidine based lymphocyte proliferation assays were performed as described previously (25); this method of measuring cell proliferation was used because the limited numbers of lymphocytes isolated from the tumor samples meant that CFSE dilution experiments were not feasible. Interferon-γ enzyme-linked immunospot (ELISPOT) assays were conducted as before (26) with co-cultures of tumoral Tregs, effector T cells and $CD3^+$ cell depleted irradiated autologous PBMCs stimulated as above. For experiments with anti-OX40 antibody, tritiated thymidine uptake and interferon-γ ELISPOT assays were performed with tumoral $CD4^+$ T cells cultured with/without anti-OX40 (5μg/ml) or mouse IgG1 (Biolegend) and stimulated as above in the presence of accessory cells.

Statistical analysis

Statistical analysis was conducted using GraphPad Prism software. For functional assays, paired Wilcoxon rank tests were used to assess significance, and for immunohistochemical and flow cytometric quantification of normally distributed data, paired T tests or one way ANOVA with Tukey's test for multiple comparisons were used.

Results

Quantification of Tregs in cSCCs

cSCCs are infiltrated by immune cells, with immunohistochemistry conducted on archived FFPE cSCCs showing accumulation of $CD3^+$ T cells in the stroma around islands of tumor keratinocytes (i.e. peritumoral), whilst $CD3^+$ T cells within tumor cell nests (i.e. intratumoral) were found less frequently (figure 1A, B and supplementary figure 1A, B). In addition to $CD4^+$ T cells and $CD8^+$ T cells within the tumoral infiltrate (i.e. combination of peritumoral and intratumoral infiltrate), frequent numbers of $CD25^+$ and $FOXP3^+$ Treg populations were also present (figure 1C, D; supplementary figure 1C, D). Quantification of the T cell subsets that comprised the tumoral immune infiltrate in 24 cSCCs demonstrated that $CD3^+$, $CD4^+$ and $CD8^+$ T cells accounted for 40.5% ± 10.3%, 36.6% ± 7.1% and 22.0% ± 7.5% of the infiltrate respectively, whilst $FOXP3^+$ Tregs comprised 11.0% ± 4.4% of the immune infiltrate, indicating a Treg to $CD4^+$ T cell ratio of approximately 1:3 and a Treg: $CD8^+$ T cell ratio of 1:2 (figure 1C). To determine whether there were differences in Treg numbers between precancerous and cancerous skin lesions, immunohistochemistry was performed which demonstrated that actinic keratoses (AKs) contained similar $FOXP3^+$ Treg frequencies to cSCCs (24.1% ± 14.2% of AK immune infiltrate versus 29.2% ± 19.4% of cSCC immune infiltrate, n=44 AKs, n=79 cSCCs, p=0.131, figure 1D).

Using anti-cytokeratin 16 to delineate the cSCC tumor islands, immunofluorescence microscopy showed the presence of $FOXP3^+$ Tregs and $CD3^+$ T cells in the stroma surrounding the cSCCs with fewer of these cells within the tumor islands (figure 1E, F). Tregs exert suppressive function via contact dependent mechanisms (27), although non-contact mechanisms may also play a role in some instances (28). Confocal microscopy of cSCCs indicated close approximation of tumoral Tregs (identified by nuclear FOXP3 and cell membrane CD4) and $CD4^+FOXP3^-$ T cells and, separately, $CD8^+$ T cells (figure 1G), suggesting contact dependent interactions between Tregs and effector T cells in this tumor. Flow cytometry of tumoral immunocytes from freshly-excised cSCCs demonstrated that cSCCs contained lower $CD4^+$ T cell frequencies than peripheral blood of the same individuals (55.7% ± 18.7% versus 70.9% ± 17.8% of the live $CD3^+$ lymphocyte population respectively, p=0.0211, n=17 tumors, figure 1H, I). By contrast, Tregs were more numerous in cSCCs than the corresponding peripheral blood and non-lesional skin (19.8% ± 8.6% versus 5.5% ± 4.1% and 7.3% ± 4.1% of the $CD4^+$ population respectively expressed FOXP3, $p<0.0001$ for both comparisons, n=86 tumors, figure 1J, K), indicating that in cSCC there is an accumulation of tumoral Tregs, potentially contributing to the protumorigenic microenvironment. Tregs were also significantly more frequent in BCC than in corresponding peripheral blood (16.7% ± 7.7% versus 2.8% ± 2.2% of $CD4^+$ population for BCC and blood respectively, p=0.0045 n=6, figure 1L). Although Tregs seemed more frequent in keratoacanthoma (KA, a skin lesion that clinically resembles cSCC but is known to regress spontaneously) than in corresponding blood (11.2% ± 7.5% versus 4.4% ± 3.3% of $CD4^+$ population for KA and blood respectively, n=6, figure 1L), there were significantly overall fewer Tregs in KA than in cSCC (p=0.0321, supplementary figure 1E).

Tregs in cSCCs are memory T cells which express the skin homing marker CLA

Many of the T cells within normal skin are effector memory T cells which express CD45RO (29). In the current study the majority of $FOXP3^+$ Tregs (87.8% ± 11.7%) and $CD4^+FOXP3^-$ T cells (85.7% ± 7.3%) in cSCCs were $CD45RO^+$ (n=8 tumors), whereas 77.6% ± 16.7% of $FOXP3^+$ Tregs and 52.7% ± 19.3% of $CD4^+FOXP3^-$ T cells in peripheral blood were $CD45RO^+$ (p=0.0171 and p=0.0013 respectively for $FOXP3^+$ Tregs and $CD4^+FOXP3^-$ T cells comparison between cSCCs and peripheral blood from same individuals, figure 2A–C). The T cell marker Helios may denote thymically derived natural Tregs (24) but can also be upregulated on activated T cells (30). Flow cytometry established that Helios was expressed at higher levels in tumoral $FOXP3^+$ Tregs (47.2% ± 7.9%, n=9 tumors) than peripheral blood $FOXP3^+$ Tregs (26.7% ± 8.5%, p=0.0022) and tumoral non-regulatory $CD4^+FOXP3^-$ T cells (9.6% ± 5.8%, p<0.0001) from the same subjects, (figure 2D, E).

Clark et al (29) have reported that T cells, including Tregs, from cSCCs lack expression of the skin homing addressins, cutaneous lymphocyte antigen (CLA) and C-C chemokine receptor 4 (CCR4). We observed that CLA was expressed by 78.8% ± 13.0% of the $FOXP3^+$ Tregs population in cSCCs, which was higher than the proportion of $FOXP3^+$ Tregs (40.0% ± 13.7%) expressing CLA in peripheral blood (p<0.0001, n=19 tumors, figure 2F, G). The latter is similar to that reported by Booth et al in blood (23). Likewise, greater numbers of $CD4^+FOXP3^-$ T cells (58.2% ± 15.1%) in cSCC expressed CLA than those in peripheral blood (p<0.0001, n=19 tumors, figure 2F, H). Furthermore, experiments performed in a separate institution on a different set of cSCCs (n=13) identified CLA positivity in 64.7% ± 31.2% of tumoral $CD3^+$ T cells (supplementary figure 2A, B). CCR4 expression was detected on 44.1% ± 32.7% of $FOXP3^+$ Tregs in cSCCs, although this was lower than the number of $FOXP3^+$ Tregs expressing CCR4 in peripheral blood (72.7% ± 17.8%), (p=0.0139, n=17 tumors, figure 2F, I). Equal numbers of tumoral $CD4^+FOXP3^-$ T cells (25.4% ± 21.4%) and peripheral blood $CD4^+FOXP3^-$ T cells (27.6% ± 19.8%) expressed CCR4 (figure 2J). Further experiments were performed to confirm the expression of CLA and CCR4 in cSCC Tregs; CCR4 was detected on cSCC Tregs at similar levels with an alternate anti-CCR4 antibody and immunofluorescence/confocal microscopy using a different anti-CLA antibody showed CLA^+ cells in cSCCs (figure 3A) and that the tumoral $FOXP3^+$ cells expressed CLA (figure 3B and supplementary figure 2C).

CLA permits lymphocyte trafficking to the skin through its binding to E-selectin on cutaneous endothelial cells (29). Immunofluorescence microscopy was performed using cytokeratin (CK) 16 or 17 co-staining which allows the cSCC tumor cells to be visualized. Blood vessels (highlighted by $CD31^+$ endothelial cells) were detected in the peritumoral areas of cSCCs with no evidence of intratumoral vessels (figure 3C and supplementary figure 3A, B), and that most of the peritumoral vasculature expressed E-selectin (figure 3D and supplementary figure 4), suggesting that CLA^+ Tregs can readily be directed to the site of the tumor from the blood via interaction with E-selectin on these endothelial cells.

cSCC Tregs suppress tumoral effector T cell responses

In vitro co-culture experiments with Tregs and effector T cells were performed to investigate cSCC Treg function. cSCC Tregs and effector T cells were co-cultured in a 1:2 ratio based on their relative frequencies observed in the prior immunohistochemical quantification experiments (figure 1C). Tumoral Tregs were identified by expression of CD3, CD4, high levels of CD25 and low levels of CD127 and isolated using fluorescence activated cell sorting (figure 4A). Sorted tumoral $CD4^+$ effector T cells identified as $CD3^+CD4^+CD25^{low}$ and $CD8^+$ effector T cells were $CD3^+CD8^+$ (figure 4A). After sorting, a sample of the cells were fixed and permeabilized for analysis of FOXP3 expression, confirming that most of the sorted $CD3^+CD4^+CD25^{high}CD127^{low}$ cells were Tregs (figure 4B and supplementary figure 5A). In addition, interferon-γ was produced by <4% of tumoral $CD3^+CD4^+CD25^{high}CD127^{low}$ cells following PMA and ionomycin stimulation, suggesting that this $CD3^+CD4^+CD25^{high}CD127^{low}$ population was minimally contaminated by effector T cells (figure 4C). Tritiated thymidine-based lymphocyte proliferation assays showed that tumoral $CD3^+CD4^+CD25^{high}CD127^{low}$ Tregs were able to suppress PHA-induced proliferation of tumoral $CD3^+CD4^+CD25^{low}$ effector T cells (median suppression 41.7%, n=10 tumors, figure 4D) and, to a lesser extent, $CD3^+CD8^+$ effector T cells (median suppression 12.6%, p=0.043, n=9 tumors, figure 4E). Tumoral Tregs also suppressed proliferation of anti-CD3 stimulated tumoral $CD4^+$ effector T cells (median suppression 46.2%, n=4 tumors, supplementary figure 5B) and $CD8^+$ T cells (median suppression 40.2%, n=4 tumors, supplementary figure 5C). In addition, ELISPOT assays demonstrated that tumoral Tregs reduced effector T cell interferon-γ secretion in response to PHA (median inhibition 24.2%, p=0.0186, n=11 tumors, figure 4F). These results indicate that tumoral Tregs from cSCCs can suppress tumoral effector T cell function, and may therefore contribute to an immunosuppressive milieu that prevents immune-mediated destruction of the tumor.

OX40 is expressed by cSCC Tregs and OX40 agonism enhances tumoral $CD4^+$ T cell function

As the costimulatory receptor OX40 is expressed on effector and regulatory T cells and can augment T cell receptor signaling (15–19), we next investigated whether OX40 was present on tumoral lymphocytes in cSCC. Immunofluorescence microscopy demonstrated the presence of OX40 predominantly on tumoral $FOXP3^+$ Tregs (figure 5A). Flow cytometry confirmed $FOXP3^+$ Tregs in cSCC expressed OX40 (39.3% ± 13.6% of $FOXP3^+$ Tregs), with significantly more tumoral Tregs expressing OX40 than $CD4^+FOXP3^-$ T cells and $CD8^+$ T cells in cSCCs, and $FOXP3^+$ Tregs, $CD4^+FOXP3^-$ T cells and $CD8^+$ T cells in peripheral blood ($p<0.0001$ for all comparisons, n=15 tumors, figure 5B, C and supplementary figure 5D). To assess if OX40 agonism attenuates the suppressive effects of Tregs in cSCC, we assessed the proliferation of tumoral $CD4^+$ T cells from cSCCs in the presence of an agonistic anti-OX40 mAb. The addition of anti-OX40, but not an isotype control mAb, led to enhancement of PHA-induced $CD4^+$ T cell proliferation (median increase in proliferation 45%, p=0.0098, n=10 tumors, figure 5D); proliferation of $CD4^+CD25^{high}CD127^{low}$ Tregs was not increased by anti-OX40 when cultured with PHA in the presence of accessory cells alone (isotype control = 108.5 cpm (IQR 68.0–129.5 cpm), anti-OX40 = 107 cpm (IQR 73.3–135.5 cpm), n=4 tumors, supplementary figure 5D).

Subsequently, tumoral $CD4^+CD25^{low}$ effector T cell proliferation was measured following culture with PHA ± anti-OX40 in the absence or presence of tumoral $CD4^+CD25^{high}CD127^{low}$ Tregs. In cultures containing tumoral $CD4^+CD25^{low}$ T cells without Tregs, median cell proliferation increased by 5.3% with the addition of anti-OX40 compared with isotype control, whereas in cultures containing tumoral $CD4^+CD25^{low}$ T cells and Tregs, the improvement in effector T cell function with the addition of anti-OX40 was more apparent (median increase in cell proliferation = 252.4% compared with isotype control, p=0.0313, n=5 tumors, figure 5E and supplementary figure 5E). Similar results were also observed when anti-CD3 was used as a stimulus instead of PHA, with anti-OX40 increasing tumoral effector $CD4^+$ T cell proliferation from 5474 to 6572 cpm (20.1%) when Tregs were absent, and from 2906 to 5263 cpm (81.1%), when Tregs were present, n=4 tumors (supplementary figure 5F). Furthermore, the increase in interferon-γ spot production by tumoral $CD4^+$ effector T cells with the addition of anti-OX40 was more apparent in the presence of tumoral Tregs (53.5 with isotype versus 93.7 with anti-OX40) than in the absence of tumoral Tregs (114.2 with isotype to 131.5 with anti-OX40, figure 5F). Taken in combination with the fact that OX40 was found mainly on Tregs in cSCCs, these results suggest that OX40 agonism reduces Treg-mediated suppression of tumoral $CD4^+$ T cell responses.

Increased Treg frequencies are associated with primary cSCCs which metastasize

In order to determine whether Tregs in cSCCs are associated with poorer clinical outcome, Tregs were quantified in archived FFPE primary cSCCs that had metastasized and in cSCCs that were known not to have metastasized after 5 years. As expected, histological data demonstrated differences in known prognostic factors between the metastatic and non-metastatic groups, with primary metastatic cSCCs being larger, invading deeper and being more poorly differentiated than non-metastatic cSCCs (figure 6A). Nevertheless, there were significantly higher frequencies of $FOXP3^+$ Tregs in primary cSCCs that metastasized than those that did not metastasize (49.3% ± 13.8% versus 23.5% ± 11.0% of immune infiltrate respectively, p<0.0001, n=29 and 26 tumors respectively) despite similar frequencies of $CD3^+$ T cells in both groups (figure 6B–D), suggesting that increased Treg numbers in primary cSCCs may influence the development of subsequent metastasis. OX40 expressing cells were also quantified in FFPE primary cSCCs, with increased percentages of tumoral immunocytes expressing OX40observed in primary metastatic cSCCs (17.0% ± 10.7% of immune infiltrate, n=48 tumors) than primary non-metastatic cSCCs (11.7% ± 6.9% of immune infiltrate, n=49 tumors, p=0.0041, figure 6B, E).

Discussion

Factors which predispose to skin cancer development in humans include light skin pigmentation secondary to genetic polymorphisms in genes such as *MC1R*, ultraviolet radiation (UV) exposure which causes DNA damage/gene mutation in relevant skin cells and altered/suppressed immunity (6–8, 21, 31). cSCCs have one of the highest mutational burdens compared with other tumor types (6–8) and high frequencies of UV-induced mutations could result in neoantigens that can be recognized by T cells (32). Indeed, the importance of the immune system in cSCC development is exemplified by the markedly

increased prevalence of this tumor type in immunosuppressed individuals (9). However, the fact that cSCCs are frequently accompanied by a substantial immune infiltrate in most individuals (including non-immunosuppressed subjects who constitute the majority of cSCC cases) highlighted a need to characterize this infiltrate from a functional perspective. Based on the viewpoint that local cutaneous immunity plays a key role in preventing cSCC development and that dysregulation of this local immunity may allow the expansion of neoplastic keratinocytes to go unchecked, we investigated the Treg population within cSCCs. Our findings demonstrate that the cSCC tumoral immune infiltrate contains higher Treg frequencies than peripheral blood, which is in keeping with studies indicating that Tregs may accumulate in various tumors via several mechanisms and with reports that exposure of skin to UV is conducive to the generation of Tregs (33). Functionally immunosuppressive Tregs have been reported in human cancer previously (10, 34–36) and this current study confirms that cSCC tumoral Tregs have the capacity to suppress tumoral effector T cell function *in vitro*, therefore highlighting Tregs as a mechanism by which cSCCs can avoid destruction by the skin immune system. In addition, higher Treg frequencies were found to be associated with primary cSCCs which had metastasized rather than primary cSCCs which had not metastasized, indicating that Tregs may play a role in allowing cSCC to metastasize and thus are of potential prognostic importance.

This study showed no difference in Treg numbers between actinic keratoses and cSCC, as reported previously (37), suggesting that Tregs accumulate during a precursor lesion stage, i.e. actinic keratoses, rather than being a determinant of progression from actinic keratosis to cSCC. However, we found an association between higher Treg frequencies in primary cSCCs and subsequent metastasis, in keeping with studies in other cancer types where Tregs have been shown to promote metastasis and influence clinical outcome (10–13, 38–40). Related to this, although we found an association between the histological differentiation status of cSCC and Treg infiltration, which was similar to a recent study (41), the association did not remain after excluding cSCCs with known clinical outcome (i.e. had metastasized or not metastasized at five years) (supplementary figure 6), suggesting a more robust association was present between Treg infiltration and metastasis than that with cSCC differentiation status in our study.

Although Gelb et al reported that lymphocytes infiltrating cSCC express CLA (42), a more recent investigation recorded that T cells infiltrating cSCCs are non-cutaneous central memory T cells which lack expression of CLA and CCR4 (29). Our phenotypic characterization of tumoral Tregs in cSCC showed that most expressed CD45RO and CLA, indicating a skin resident memory phenotype (which is the predominant T cell phenotype in skin) in cSCCs. We confirmed the expression of CLA on cSCC Tregs using both flow cytometry and immunofluorescence microscopy with two different anti-CLA antibodies (from BD Biosciences and Biolegend). However, our results demonstrate a high degree of variability in CLA and CCR4 expression between tumors, suggesting heterogeneous T cell responses in cSCC, possibly accounting for the differences between previous studies. In the context of the E-selectin expression by the majority of the peritumoral blood vessels, our findings signify that Tregs are generally recruited to cSCCs via CLA on the Treg surface interacting with E-selectin on the tumoral vasculature. This is akin to T cell recruitment in

inflammatory skin conditions including psoriasis (43), atopic dermatitis (44) and contact dermatitis (45) as well as in other cutaneous neoplasms such as melanoma (42).

There has been considerable interest in developing cancer treatments that use monoclonal antibodies which act on T cell costimulatory pathways to augment antitumor immunity (15–20). Indeed, effector T cell responses can be modulated through engaging costimulatory receptors which can attenuate Treg suppressive ability (15–19, 46). *In vitro* studies of human peripheral blood T cells have demonstrated that anti-OX40 mAbs can be agonistic which can enhance the resistance of effector T cells to suppression and reduce the suppressive activity of Tregs (19). In addition, anti-OX40 mAbs could stimulate anti-tumor immunity by preferential depletion of Tregs, as shown in pre-clinical studies (17, 18). Furthermore, a phase I clinical trial using an anti-OX40 agonistic monoclonal antibody has shown an acceptable safety/toxicity profile and some evidence of tumor regression in cases of melanoma, renal cancer, urethral squamous cell carcinoma, prostate cancer and cholangiocarcinoma (20). In our study, the tumoral Tregs were the T cell subset that expressed OX40 at the highest frequencies, consistent with observations from studies on murine tumors which used anti-OX40 antibodies to deplete intratumoral Tregs and enhance anti-tumor immunity (16–18), suggesting a similar strategy could be beneficial in cSCC. OX40 has been demonstrated on $CD4^+$ tumor-infiltrating lymphocytes in melanoma and head and neck cancer (47), and whereas a recent study has documented the presence of OX40 expressing lymphocytes in cSCC (48), our work highlights that this molecule is predominantly expressed by Tregs in this cancer. Furthermore, our study shows that higher percentages of tumor infiltrating lymphocytes express OX40 in primary metastasizing cSCCs compared with primary tumors which had not metastasized. While this contrasts with some other cancers in which OX40 expression correlates with improved prognosis (49–51), much higher proportions of tumoral Tregs expressed OX40 than the tumoral $CD4^+FOXP3^-$ and $CD8^+$ T cells in our cSCC population. Furthermore, using an *in vitro* culture model, enhanced tumoral $CD4^+$ T cell responses were observed with addition of an OX40 agonist, suggesting that the use of an OX40 agonist approach *in vivo* may have potential benefits in patients with cSCCs at high risk of metastasizing after surgical excision. Admittedly, although OX40 agonism had little effect on enhancing proliferation of tumoral $CD4^+$ effector T cells and interferon-γ production in the absence of Tregs, it is unclear whether part of the effect of OX40 agonism could be mediated by the presence of $OX40^+FOXP3^-$ cells in the sorted $CD3^+CD4^+CD25^{high}CD127^{low}$ population (supplementary figure 5D). This is because, due to FOXP3 being an intracellular stain, it was not possible to isolate the $FOXP3^-$ fraction of the $CD3^+CD4^+CD25^{high}CD127^{low}$ population from human cSCCs and perform functional studies using this subset alone. Neither is it clear whether the effect of OX40 agonism is mediated by $OX40^+CD4^+$ effector T cells in overcoming or influencing Treg suppression, however, our results indicate that the effect of OX40 agonism in boosting the effector T cell response is only seen in the presence of the $CD3^+CD4^+CD25^{high}CD127^{low}$ Treg population.

In conclusion, this study demonstrates that cSCCs contain an abundance of Tregs which can suppress tumoral effector T cell function and that activation of the costimulatory receptor OX40 enhances tumoral T cell responses. Primary cSCCs that metastasize are associated

with higher Treg frequencies, therefore providing evidence that Tregs play a key role in the pathogenesis of cSCC.

Supplementary Material

Refer to Web version on PubMed Central for supplementary material.

Acknowledgments

The authors would like to thank Richard Jewell and Carolann McGuire in Dermatopharmacology, University of Southampton; Ian Mockeridge and Dima Taraban in Cancer Sciences, University of Southampton; Susan Wilson and Jon Ward from the Histochemistry Research Unit, University of Southampton; and Dave Johnston from the Biomedical Imaging Unit, University of Southampton for their technical support. We are also grateful to Trevor Bryant and Scott Harris, Medical Statistics, University of Southampton, for providing statistical advice. In addition, we would like to thank the administrative and nursing staff, including Margaret Wheeler and Amanda Clowes, in the Dermatology Department, University Hospital Southampton NHS Foundation Trust for assistance with procurement of samples from patients.

Financial support: CL is supported by a Wellcome Trust Research Training Fellowship. Support was also provided from National Institute for Health Research Academic Clinical Fellowships (CL, SA, SYC), the Ministry of Higher Education and Scientific Research – Libya (AA) and Cancer Research UK (RRF, AAl-S, MJG). ASM is supported by a National Institutes of Health K08 award (5K08 AR063729) and by the Skin Disease Research Center at Duke University.

References

1. Lucas, R.; McMichael, T.; Smith, W.; Armstrong, B. Solar ultraviolet radiation: Global burden of disease from solar ultraviolet radiation. Geneva: World Health Organization Public Health and the Environment; 2006.
2. Rogers HW, Weinstock MA, Harris AR, Hinckley MR, Feldman SR, Fleischer AB, et al. Incidence estimate of nonmelanoma skin cancer in the United States, 2006. Arch Dermatol. 2010; 146:283–7. [PubMed: 20231499]
3. Bickers DR, Lim HW, Margolis D, Weinstock MA, Goodman C, Faulkner E, et al. The burden of skin diseases: 2004 a joint project of the American Academy of Dermatology Association and the Society for Investigative Dermatology. J Am Acad Dermatol. 2006; 55:490–500. [PubMed: 16908356]
4. Alam M, Ratner D. Cutaneous squamous-cell carcinoma. N Engl J Med. 2001; 344:975–83. [PubMed: 11274625]
5. Brantsch KD, Meisner C, Schonfisch B, Trilling B, Wehner-Caroli J, Rocken M, et al. Analysis of risk factors determining prognosis of cutaneous squamous-cell carcinoma: a prospective study. Lancet Oncol. 2008; 9:713–20. [PubMed: 18617440]
6. Durinck S, Ho C, Wang NJ, Liao W, Jakkula LR, Collisson EA, et al. Temporal dissection of tumorigenesis in primary cancers. Cancer Discov. 2011; 1:137–43. [PubMed: 21984974]
7. Li YY, Hanna GJ, Laga AC, Haddad RI, Lorch JH, Hammerman PS. Genomic analysis of metastatic cutaneous squamous cell carcinoma. Clin Cancer Res. 2015; 21:1447–56. [PubMed: 25589618]
8. Pickering CR, Zhou JH, Lee JJ, Drummond JA, Peng SA, Saade RE, et al. Mutational landscape of aggressive cutaneous squamous cell carcinoma. Clin Cancer Res. 2014; 20:6582–92. [PubMed: 25303977]
9. Euvrard S, Kanitakis J, Claudy A. Skin cancers after organ transplantation. N Engl J Med. 2003; 348:1681–91. [PubMed: 12711744]
10. Curiel TJ, Coukos G, Zou L, Alvarez X, Cheng P, Mottram P, et al. Specific recruitment of regulatory T cells in ovarian carcinoma fosters immune privilege and predicts reduced survival. Nat Med. 2004; 10:942–9. [PubMed: 15322536]
11. Deng L, Zhang H, Luan Y, Zhang J, Xing Q, Dong S, et al. Accumulation of foxp3+ T regulatory cells in draining lymph nodes correlates with disease progression and immune suppression in colorectal cancer patients. Clin Cancer Res. 2010; 16:4105–12. [PubMed: 20682706]

12. Bates GJ, Fox SB, Han C, Leek RD, Garcia JF, Harris AL, et al. Quantification of regulatory T cells enables the identification of high-risk breast cancer patients and those at risk of late relapse. J Clin Oncol. 2006; 24:5373–80. [PubMed: 17135638]
13. Ichihara F, Kono K, Takahashi A, Kawaida H, Sugai H, Fujii H. Increased populations of regulatory T cells in peripheral blood and tumor-infiltrating lymphocytes in patients with gastric and esophageal cancers. Clin Cancer Res. 2003; 9:4404–8. [PubMed: 14555512]
14. Simpson TR, Li F, Montalvo-Ortiz W, Sepulveda MA, Bergerhoff K, Arce F, et al. Fc-dependent depletion of tumor-infiltrating regulatory T cells co-defines the efficacy of anti-CTLA-4 therapy against melanoma. J Exp Med. 2013; 210:1695–710. [PubMed: 23897981]
15. Taraban VY, Rowley TF, O'Brien L, Chan HT, Haswell LE, Green MH, et al. Expression and costimulatory effects of the TNF receptor superfamily members CD134 (OX40) and CD137 (4-1BB), and their role in the generation of anti-tumor immune responses. Eur J Immunol. 2002; 32:3617–27. [PubMed: 12516549]
16. Piconese S, Valzasina B, Colombo MP. OX40 triggering blocks suppression by regulatory T cells and facilitates tumor rejection. J Exp Med. 2008; 205:825–39. [PubMed: 18362171]
17. Marabelle A, Kohrt H, Sagiv-Barfi I, Ajami B, Axtell RC, Zhou G, et al. Depleting tumor-specific Tregs at a single site eradicates disseminated tumors. J Clin Invest. 2013; 123:2447–63. [PubMed: 23728179]
18. Bulliard Y, Jolicoeur R, Zhang J, Dranoff G, Wilson NS, Brogdon JL. OX40 engagement depletes intratumoral Tregs via activating FcgammaRs, leading to antitumor efficacy. Immunol Cell Biol. 2014; 92:475–80. [PubMed: 24732076]
19. Voo KS, Bover L, Harline ML, Vien LT, Facchinetti V, Arima K, et al. Antibodies targeting human OX40 expand effector T cells and block inducible and natural regulatory T cell function. J Immunol. 2013; 191:3641–50. [PubMed: 24014877]
20. Curti BD, Kovacsovics-Bankowski M, Morris N, Walker E, Chisholm L, Floyd K, et al. OX40 is a potent immune-stimulating target in late-stage cancer patients. Cancer Res. 2013; 73:7189–98. [PubMed: 24177180]
21. Robinson S, Dixon S, August S, Diffey B, Wakamatsu K, Ito S, et al. Protection against UVR involves MC1R-mediated non-pigmentary and pigmentary mechanisms in vivo. J Invest Dermatol. 2010; 130:1904–13. [PubMed: 20237490]
22. Pickard C, Louafi F, McGuire C, Lowings K, Kumar P, Cooper H, et al. The cutaneous biochemical redox barrier: a component of the innate immune defenses against sensitization by highly reactive environmental xenobiotics. J Immunol. 2009; 183:7576–84. [PubMed: 19890059]
23. Booth NJ, McQuaid AJ, Sobande T, Kissane S, Agius E, Jackson SE, et al. Different proliferative potential and migratory characteristics of human CD4+ regulatory T cells that express either CD45RA or CD45RO. J Immunol. 2010; 184:4317–26. [PubMed: 20231690]
24. Thornton AM, Korty PE, Tran DQ, Wohlfert EA, Murray PE, Belkaid Y, et al. Expression of Helios, an Ikaros transcription factor family member, differentiates thymic-derived from peripherally induced Foxp3+ T regulatory cells. J Immunol. 2010; 184:3433–41. [PubMed: 20181882]
25. Cooper A, Robinson SJ, Pickard C, Jackson CL, Friedmann PS, Healy E. Alpha-melanocyte-stimulating hormone suppresses antigen-induced lymphocyte proliferation in humans independently of melanocortin 1 receptor gene status. J Immunol. 2005; 175:4806–13. [PubMed: 16177130]
26. Newell L, Polak ME, Perera J, Owen C, Boyd P, Pickard C, et al. Sensitization via healthy skin programs Th2 responses in individuals with atopic dermatitis. J Invest Dermatol. 2013; 133:2372–80. [PubMed: 23528819]
27. Gondek DC, Lu LF, Quezada SA, Sakaguchi S, Noelle RJ. Cutting edge: contact-mediated suppression by CD4+CD25+ regulatory cells involves a granzyme B-dependent, perforin-independent mechanism. J Immunol. 2005; 174:1783–6. [PubMed: 15699103]
28. Delgoffe GM, Woo SR, Turnis ME, Gravano DM, Guy C, Overacre AE, et al. Stability and function of regulatory T cells is maintained by a neuropilin-1-semaphorin-4a axis. Nature. 2013; 501:252–6. [PubMed: 23913274]

29. Clark RA, Huang SJ, Murphy GF, Mollet IG, Hijnen D, Muthukuru M, et al. Human squamous cell carcinomas evade the immune response by down-regulation of vascular E-selectin and recruitment of regulatory T cells. J Exp Med. 2008; 205:2221–34. [PubMed: 18794336]

30. Gottschalk RA, Corse E, Allison JP. Expression of Helios in peripherally induced Foxp3+ regulatory T cells. J Immunol. 2012; 188:976–80. [PubMed: 22198953]

31. Healy E, Flannagan N, Ray A, Todd C, Jackson IJ, Matthews JN, et al. Melanocortin-1-receptor gene and sun sensitivity in individuals without red hair. Lancet. 2000; 355:1072–3. [PubMed: 10744096]

32. Linnemann C, van Buuren MM, Bies L, Verdegaal EM, Schotte R, Calis JJ, et al. High-throughput epitope discovery reveals frequent recognition of neo-antigens by CD4+ T cells in human melanoma. Nat Med. 2015; 21:81–5. [PubMed: 25531942]

33. Yamazaki S, Nishioka A, Kasuya S, Ohkura N, Hemmi H, Kaisho T, et al. Homeostasis of thymus-derived Foxp3+ regulatory T cells is controlled by ultraviolet B exposure in the skin. J Immunol. 2014; 193:5488–97. [PubMed: 25348622]

34. Gobert M, Treilleux I, Bendriss-Vermare N, Bachelot T, Goddard-Leon S, Arfi V, et al. Regulatory T cells recruited through CCL22/CCR4 are selectively activated in lymphoid infiltrates surrounding primary breast tumors and lead to an adverse clinical outcome. Cancer Res. 2009; 69:2000–9. [PubMed: 19244125]

35. Jie HB, Gildener-Leapman N, Li J, Srivastava RM, Gibson SP, Whiteside TL, et al. Intratumoral regulatory T cells upregulate immunosuppressive molecules in head and neck cancer patients. Br J Cancer. 2013; 109:2629–35. [PubMed: 24169351]

36. Pedroza-Gonzalez A, Verhoef C, Ijzermans JN, Peppelenbosch MP, Kwekkeboom J, Verheij J, et al. Activated tumor-infiltrating CD4+ regulatory T cells restrain antitumor immunity in patients with primary or metastatic liver cancer. Hepatology. 2013; 57:183–94. [PubMed: 22911397]

37. Muhleisen B, Petrov I, Gachter T, Kurrer M, Scharer L, Dummer R, et al. Progression of cutaneous squamous cell carcinoma in immunosuppressed patients is associated with reduced CD123+ and FOXP3+ cells in the perineoplastic inflammatory infiltrate. Histopathology. 2009; 55:67–76. [PubMed: 19614769]

38. Lee HE, Park DJ, Kim WH, Kim HH, Lee HS. High FOXP3+ regulatory T-cell density in the sentinel lymph node is associated with downstream non-sentinel lymph-node metastasis in gastric cancer. Br J Cancer. 2011; 105:413–9. [PubMed: 21730981]

39. Tan W, Zhang W, Strasner A, Grivennikov S, Cheng JQ, Hoffman RM, et al. Tumour-infiltrating regulatory T cells stimulate mammary cancer metastasis through RANKL-RANK signalling. Nature. 2011; 470:548–53. [PubMed: 21326202]

40. deLeeuw RJ, Kost SE, Kakal JA, Nelson BH. The prognostic value of FoxP3+ tumor-infiltrating lymphocytes in cancer: a critical review of the literature. Clin Cancer Res. 2012; 18:3022–9. [PubMed: 22510350]

41. Azzimonti B, Zavattaro E, Provasi M, Vidali M, Conca A, Catalano E, et al. Intense Foxp3+ CD25+ regulatory T-cell infiltration is associated with high-grade cutaneous squamous cell carcinoma and counterbalanced by CD8+/Foxp3+ CD25+ ratio. Br J Dermatol. 2015; 172:64–73. [PubMed: 24910265]

42. Gelb AB, Smoller BR, Warnke RA, Picker LJ. Lymphocytes infiltrating primary cutaneous neoplasms selectively express the cutaneous lymphocyte-associated antigen (CLA). Am J Pathol. 1993; 142:1556–64. [PubMed: 7684198]

43. Lowes MA, Suarez-Farinas M, Krueger JG. Immunology of psoriasis. Annu Rev Immunol. 2014; 32:227–55. [PubMed: 24655295]

44. Islam SA, Luster AD. T cell homing to epithelial barriers in allergic disease. Nat Med. 2012; 18:705–15. [PubMed: 22561834]

45. Cavani A, Nasorri F, Ottaviani C, Sebastiani S, De Pita O, Girolomoni G. Human CD25+ regulatory T cells maintain immune tolerance to nickel in healthy, nonallergic individuals. J Immunol. 2003; 171:5760–8. [PubMed: 14634084]

46. Taraban VY, Slebioda TJ, Willoughby JE, Buchan SL, James S, Sheth B, et al. Sustained TL1A expression modulates effector and regulatory T-cell responses and drives intestinal goblet cell hyperplasia. Mucosal Immunol. 2011; 4:186–96. [PubMed: 20962771]

47. Vetto JT, Lum S, Morris A, Sicotte M, Davis J, Lemon M, et al. Presence of the T-cell activation marker OX-40 on tumor infiltrating lymphocytes and draining lymph node cells from patients with melanoma and head and neck cancers. Am J Surg. 1997; 174:258–65. [PubMed: 9324133]

48. Feldmeyer L, Ching G, Vin H, Ma W, Bansal V, Chitsazzadeh V, et al. Differential T-cell Subset Representation in Cutaneous Squamous Cell Carcinoma Arising in Immunosuppressed vs. Immunocompetent Individuals. Exp Dermatol. 2015 Oct 17. Epub ahead of print. doi: 10.1111/exd.12878

49. Sarff M, Edwards D, Dhungel B, Wegmann KW, Corless C, Weinberg AD, et al. OX40 (CD134) expression in sentinel lymph nodes correlates with prognostic features of primary melanomas. Am J Surg. 2008; 195:621–5. discussion 5. [PubMed: 18374895]

50. Petty JK, He K, Corless CL, Vetto JT, Weinberg AD. Survival in human colorectal cancer correlates with expression of the T-cell costimulatory molecule OX-40 (CD134). Am J Surg. 2002; 183:512–8. [PubMed: 12034383]

51. Ladanyi A, Somlai B, Gilde K, Fejos Z, Gaudi I, Timar J. T-cell activation marker expression on tumor-infiltrating lymphocytes as prognostic factor in cutaneous malignant melanoma. Clin Cancer Res. 2004; 10:521–30. [PubMed: 14760073]

Translational relevance

Cutaneous squamous cell carcinoma (cSCC) is a highly prevalent cancer which is capable of metastasizing despite treatment by surgical excision. Alterations in immunity greatly influence cancer development, especially cSCC development. As cSCCs are heavily infiltrated with T cells, cSCCs form an attractive model to study cancer T cell immunology. In this study, increased Treg frequencies were identified in cSCCs compared with peripheral blood. Moreover, tumoral Tregs suppressed tumoral effector T cell responses *in vitro*, indicating a role for Tregs in preventing effector T cell response against this tumor. Significantly more Tregs were observed in primary cSCCs which had metastasized than in primary cSCCs which had not metastasized, suggesting that tumoral Tregs may influence clinical outcome in this tumor. Additionally, an agonistic anti-OX40 antibody enhanced tumoral $CD4^+$ effector T cell responses *in vitro*, supporting a rationale for investigating OX40 activation as a potential immunotherapeutic strategy for cSCC.

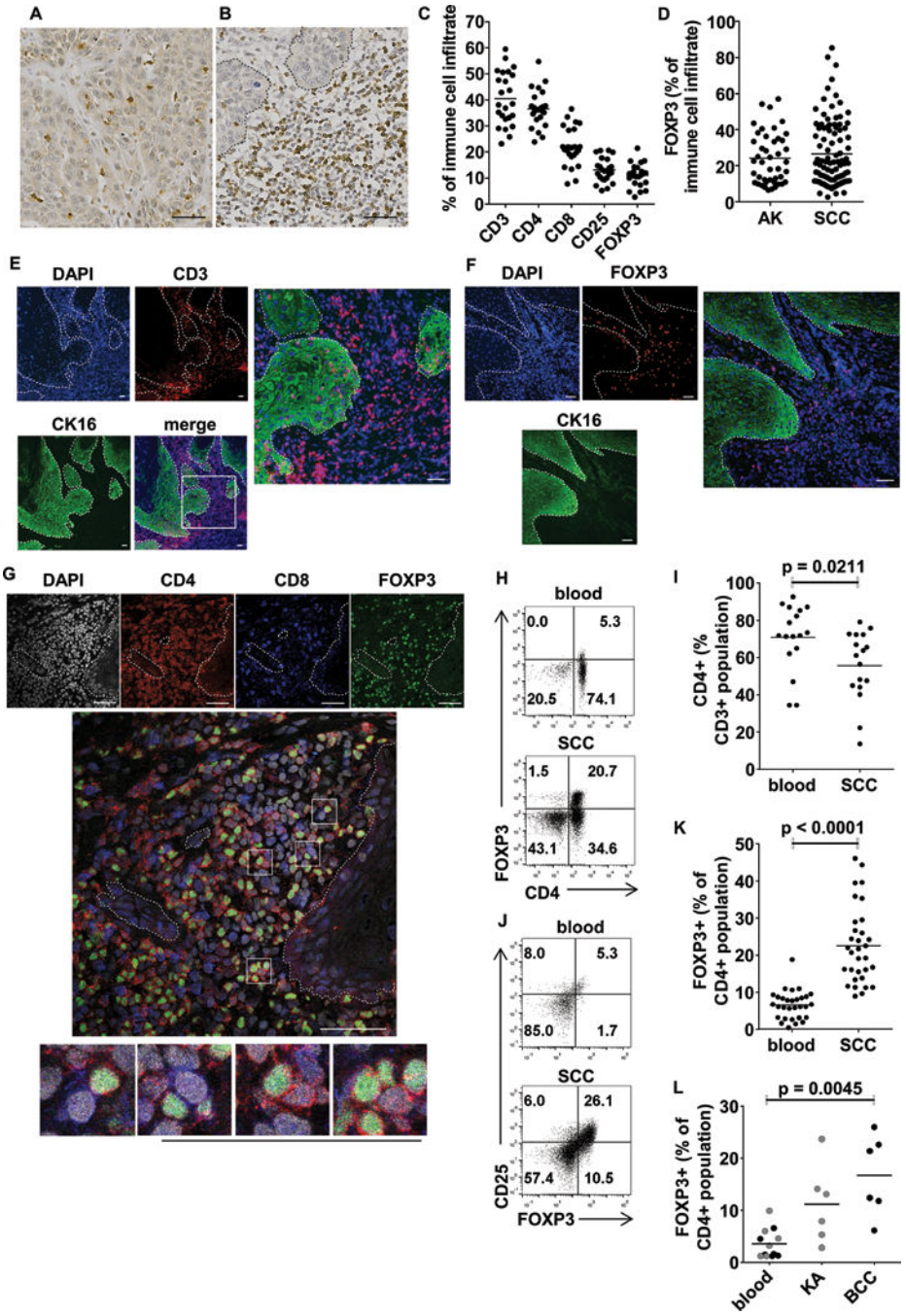

Figure 1.

Tregs accumulate in cSCC and cluster with $CD4^+$ and $CD8^+$ T cells predominantly in the peritumoral stroma. Immunohistochemistry of cSCC demonstrating $CD3^+$ T cells in (A) intratumoral and (B) peritumoral areas. (C) Immunohistochemical quantification of T cell subsets in 24 cSCCs. (D) No differences in frequencies of infiltrating $FOXP3^+$ cells were observed between actinic keratoses (AKs, n=44) and cSCCs (n=79). Immunofluorescence staining demonstrating (E) $CD3^+$ T cells and (F) $FOXP3^+$ Tregs in cSCC. Cytokeratin (CK) 16 staining highlights tumor keratinocytes. (G) Confocal microscopy of $CD4^+$ T cells, $CD8^+$

T cells and $CD4^+FOXP3^+$ T cells in cSCC, boxes highlight examples of $CD4^+FOXP3^+$ Tregs (red membrane, green nucleus) in close contact with $CD8^+$ T cells (blue membrane, grey nucleus) and $CD4^+FOXP3^-$ T cells (red membrane, grey nucleus). (H) Flow cytometry plots of $CD3^+$ gated lymphocytes isolated from peripheral blood and matched cSCC demonstrating CD4 and FOXP3 expression. (I) Aggregate data showing fewer $CD4^+$ T cells as a proportion of the $CD3^+$ population in cSCCs compared with blood (n=17). (J) $CD3^+CD4^+$ gated lymphocyte populations in blood and corresponding cSCC plotted for FOXP3 and CD25 expression. (K) Data from 32 cSCCs demonstrating higher $FOXP3^+$ Treg frequencies as a percentage of the $CD4^+$ T cell population in cSCC than blood. (L) $FOXP3^+$ Treg frequencies in keratoacanthoma (KA), basal cell carcinoma (BCC) and corresponding blood. In images A, B, E, F & G, scale bars = 50 μm, dashed lines indicate tumor outlines. In graphs C & D, dots = mean cell frequencies in 5 separate 40× fields for each lesion, horizontal bars = mean values for all lesions. In graphs I – L, horizontal bars = means.

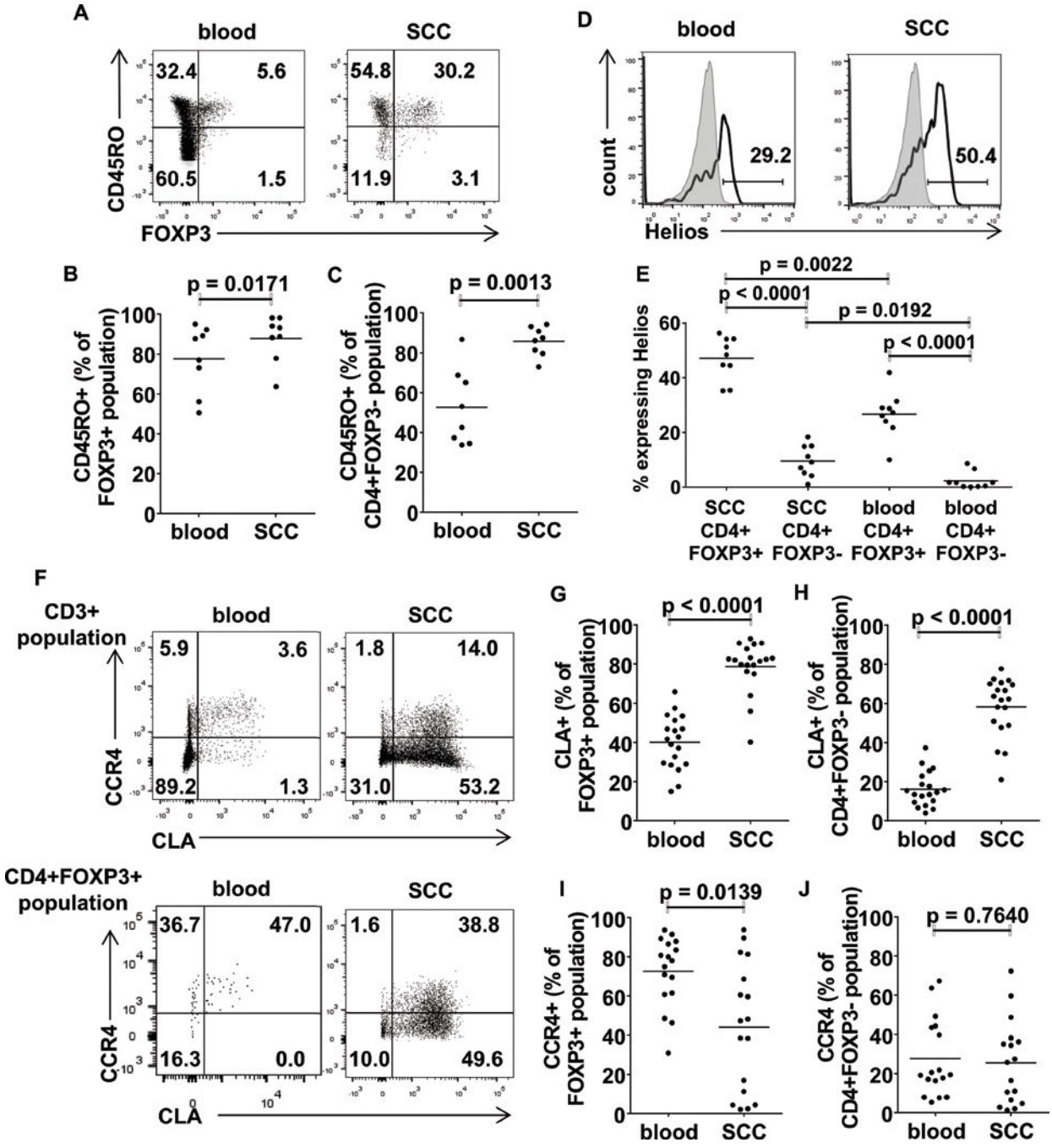

Figure 2.

Phenotypic characterization of cSCC Tregs. (A) FACS plots showing CD45RO expression on $CD3^+CD4^+$ gated lymphocyte populations from peripheral blood and cSCC. CD45RO positivity as a percentage of (B) $CD4^+FOXP3^+$ Treg and (C) $CD4^+FOXP3^-$ T cell populations from blood and cSCC (n=8), showing that these populations in cSCCs are mainly $CD45RO^+$ memory T cells. (D) Representative histograms demonstrating Helios expression in $CD3^+CD4^+FOXP3^+$ gated lymphocytes from peripheral blood and corresponding cSCC. Grey shaded areas represent isotype control. (E) Percentage of tumoral

$CD4^+FOXP3^+$ Tregs, tumoral $CD4^+FOXP3^-$ T cells and peripheral blood $CD4^+FOXP3^+$ Tregs that are $Helios^+$ (n=9). (F) Representative plots demonstrating CLA and CCR4 expression in $CD3^+$ and $CD3^+CD4^+FOXP3^+$ gated lymphocytes from peripheral blood and cSCC from the same subject. Graphs showing aggregate data for CLA expression in peripheral blood and tumoral (G) $CD3^+CD4^+FOXP3^+$ Tregs and (H) $CD3^+CD4^+FOXP3^-$ T cells (n=19), and CCR4 expression in peripheral blood and tumoral (I) $CD3^+CD4^+FOXP3^+$ Tregs and (J) $CD3^+CD4^+FOXP3^-$ T cells (n=19). Horizontal bars on graphs B, C, E, G, H, I & J = means.

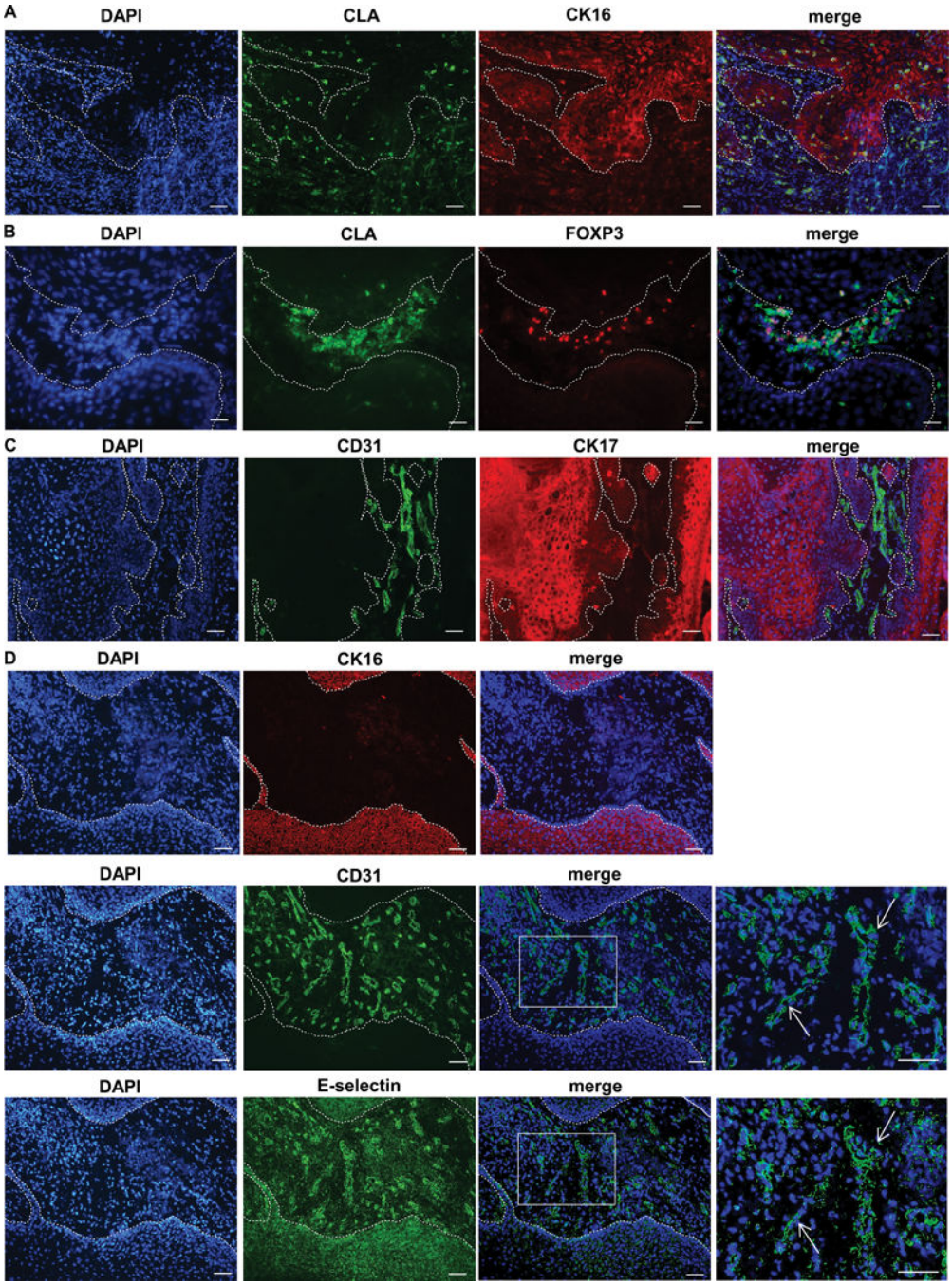

Figure 3.

cSCC Tregs express the skin homing marker CLA. (A) Immunofluorescence microscopy of cSCC cryosections showing CLA^+ tumoral immunocytes, cytokeratin (CK) 16 highlights tumor keratinocytes. (B) Immunofluorescence microscopy demonstrating CLA^+ $FOXP3^+$ Tregs in cSCC. (C) $CD31^+$ staining highlighting peritumoral blood vessels in cSCC stroma, cytokeratin (CK) 17 positivity indicates tumor keratinocytes. (D) Sequential cSCC sections showing e-selectin expression in the peritumoral vasculature (highlighted by CD31 straining) between cytokeratin (CK) 16 positive tumor islands. Arrows in the right hand

boxes, which depict higher power images of the merged images, indicate the same blood vessels in sequential sections. Dashed lines represent the outlines of the tumor in A – D, scale bars = 50 μm.

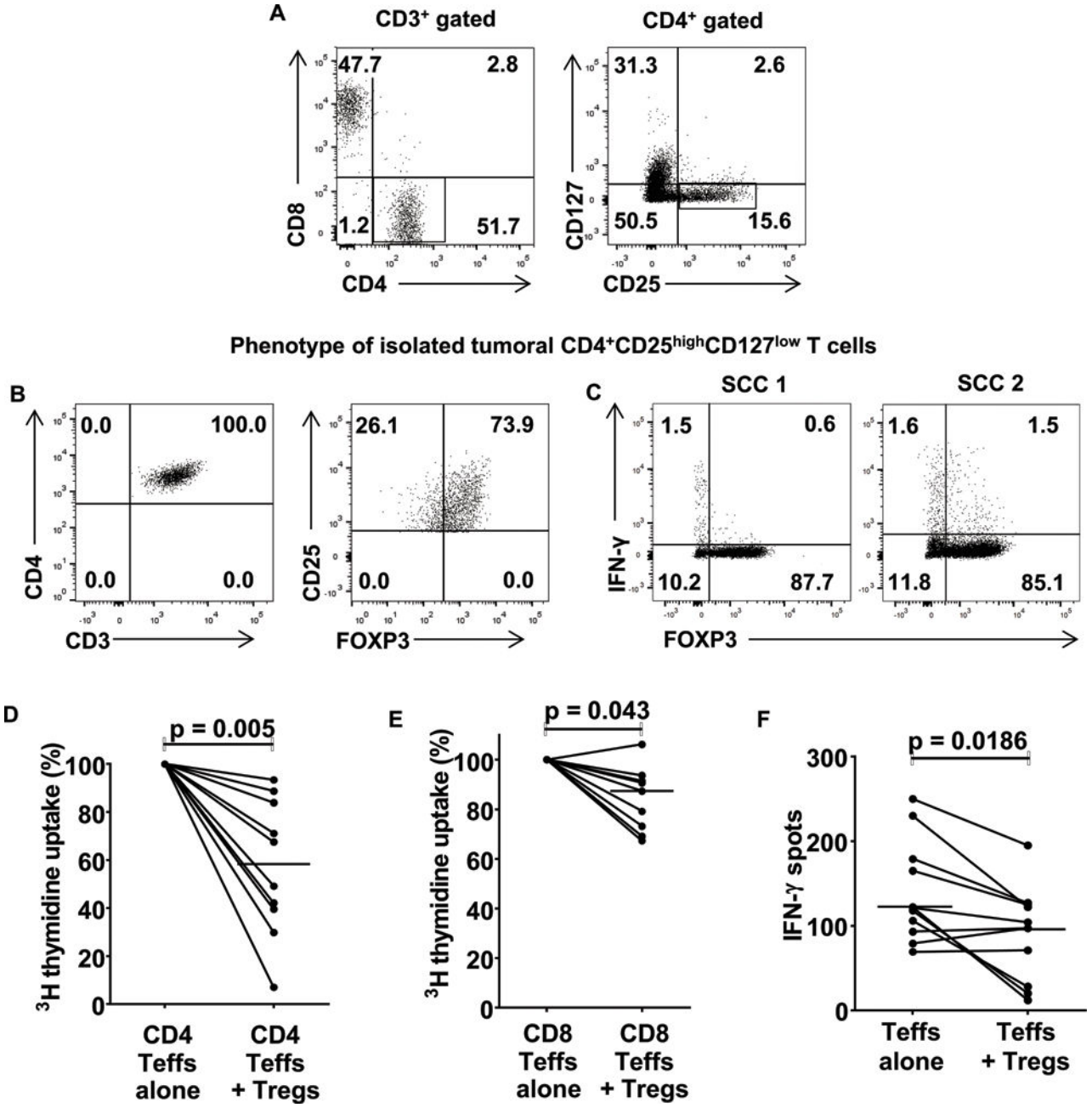

Figure 4.

cSCC Tregs suppress PHA-induced tumoral effector T cell responses *in vitro*. (A) Representative flow cytometry gating strategy for isolating cSCC Tregs and effector T cells. Highlighted box in the left FACS plot shows the $CD3^+CD4^+$ population, and sub-gating of this population is displayed in the right FACS plot, where the sorted $CD25^{high}CD127^{low}$ Treg population is shown in the highlighted area. Effector T cells were $CD3^+CD4^+CD25^{low}$ or $CD3^+CD8^+$. (B) The majority of sorted $CD3^+CD4^+CD25^{high}CD127^{low}$ cells expressed FOXP3, consistent with their Treg status. (C) Sorted $CD3^+CD4^+CD25^{high}CD127^{low}$ cells were stimulated with PMA and ionomycin for 5 hours and intracellular flow cytometry was performed for FOXP3 and interferon-γ. (D–F) Tumoral effector T cells were co-cultured in

the presence of autologous irradiated PBMCs and 1μg/ml PHA with/without the addition of tumoral Tregs. Tritiated thymidine uptake was used to assess (C) tumoral $CD4^+$ T cell proliferation, n=10 tumors, (D) tumoral $CD8^+$ T cell proliferation, n=9 tumors and ELISPOT assays to determine (E) tumoral effector T cell interferon-γ secretion, n=11 tumors. In C–E, dots = median values for each tumor from triplicate well experiments, horizontal bars = median values for all tumors.

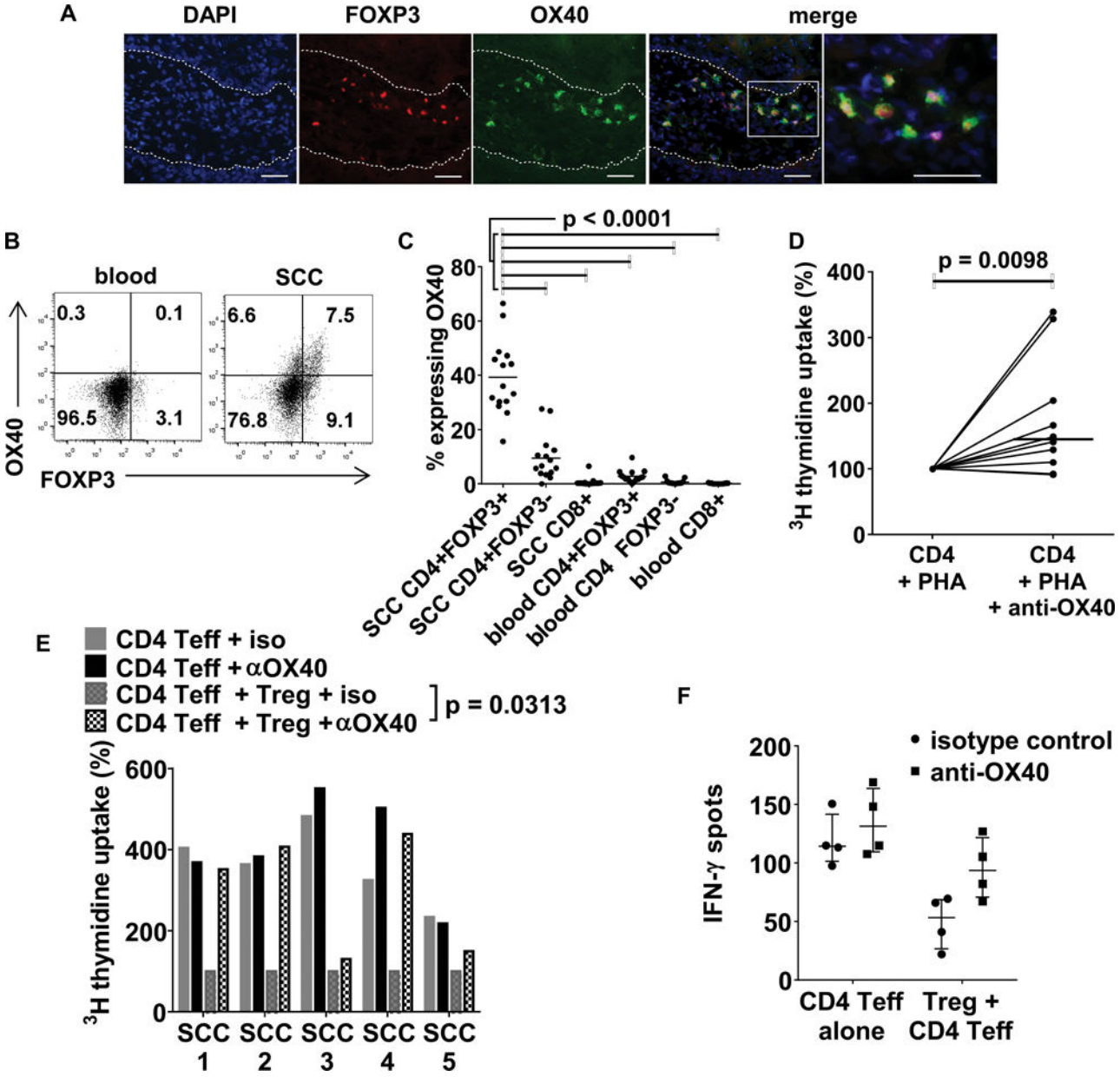

Figure 5.

OX40 is expressed by Tregs in cSCC and *in vitro* OX40 activation enhances tumoral $CD4^+$ T cell proliferation. (A) Immunofluorescence microscopy showing OX40 on tumoral $FOXP3^+$ Tregs. Dashed lines indicate the outline of the cSCC tumor islands, scale bars = 50 μm. (B) Flow cytometry plots of $CD3^+CD4^+$ gated lymphocytes from cSCC and corresponding peripheral blood showing OX40 and FOXP3 expression. (C) FACS quantification of OX40 expression in tumoral Tregs, tumoral effector T cells and peripheral blood Tregs, n=15 tumors, horizontal bars=means. (D) Tumoral $CD4^+$ T cells isolated by flow cytometry from 10 fresh cSCCs were cultured with 1μg/ml PHA + autologous irradiated $CD3^+$ cell depleted irradiated PBMCs ± agonistic anti-OX40 antibody (5μg/ml). Proliferation was assessed by tritiated thymidine uptake, dots = median values from

triplicate wells for each tumor, horizontal bar = median value from all tumors. (E) Tritiated thymidine uptake assays were performed where tumoral $CD4^+$ effector T cells were cultured ± tumoral Tregs ± agonistic anti-OX40 antibody. Median values from triplicate wells are shown and represented as normalized to 100% of CD4 Teff + Treg + iso, n=5 tumors. (F) interferon-γ ELISPOT assays, showing that the effect of the agonistic OX40 antibody is more apparent when tumoral Tregs are present in culture. Dots/circles = median values for each tumor with circles for isotype control, squares for anti-OX40, horizontal bar = median for all tumors, error bars = IQR, n=4 tumors.

A

	Primary non metastatic	Primary metastatic
Age (years)	74.8 ± 10.3	80.0 ± 10.6
Male	71.4%	77.1%
Female	28.6%	22.9%
Tumor diameter (mm)	13.4 ± 8.7	29.0 ± 30.5
Tumor depth (mm)	4.1 ± 2.7	7.9 ± 5.9
Well differentiated	34.7%	2.1%
Moderately differentiated	55.1%	29.2%
Poorly differentiated	10.2%	68.8%
Perivascular invasion	2.0%	20.1%
Perineural invasion	4.1%	25.0%
Immunosuppressed	8.2%	16.3%
Fully excised	100%	87.5%

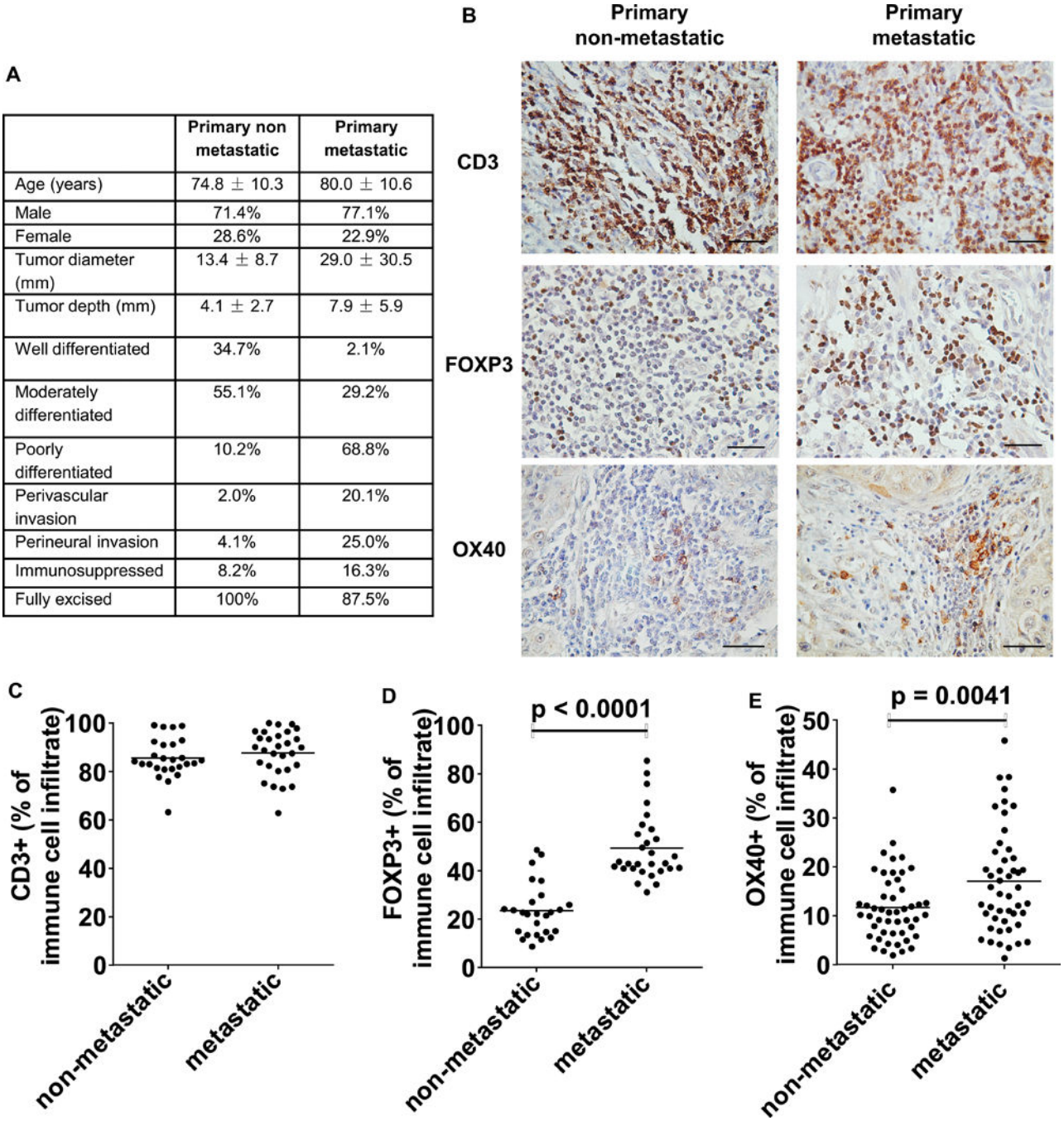

Figure 6.

Higher numbers of tumoral Tregs are associated with subsequent development of metastasis from primary cSCCs. Immunohistochemistry was conducted on archived FFPE sections of primary cSCCs that had not metastasized at 5 years post-excision (primary non-metastatic) and primary cSCCs which had metastasized (primary metastatic) post-excision. (A) Table showing histological details of primary non-metastatic and primary metastatic cSCCs. (B) Representative images of tumoral $CD3^+$ T cells, $FOXP3^+$ Tregs and $OX40^+$ immunocytes in primary non-metastatic and primary metastatic cSCCs, scale bars = 50 μm. Quantification of

tumoral (C) $CD3^+$ T cells, (D) $FOXP3^+$ Tregs in 26 primary non-metastatic and 29 primary metastatic cSCCs and (E) $OX40^+$ cells in 49 primary non-metastatic and 48 primary metastatic cSCCs. Dots on the graphs indicate mean values for each tumor from 5 high power fields, horizontal bars represent mean values for each group.